Project no. 248992

Project acronym: NEUNEU

Project title: Artificial Wet Neuronal Networks from Compartmentalised Excitable Chemical Media

Small or medium-scale focused research project (STREP)

Deliverable 4.8 - Report or publication on autonomous network generation through self-organization

This deliverable consists of a manuscript in preparation on following the information flow in droplet networks as well as an accepted manuscript, showing how to measure the oscillations parameters.

Start date of project: 1.2.2010 Duration: 36 months

Project coordinator name: Dr. Peter Dittrich
Project coordinator organisation name: Friedrich Schiller University Jena

Understanding Computing Droplet Networks by Following Information Flow

Gerd Gruenert[1,4], Konrad Gizynski[2,4], Gabi Escuela[1], Bashar Ibrahim[1,3], Jerzy Gorecki[2], and Peter Dittrich[1]

[1]Friedrich Schiller University Jena, Department of Computer Science, Bio Systems Analysis Group, Ernst-Abbe-Platz 2, D-07743 Jena, Germany
[2]Institute of Physical Chemistry, Polish Academy of Sciences, Kasprzaka 44/52, 01-224 Warsaw, Poland
[3]University College in Al-Qunfudah, Umm Al-Qura University, 1109 Makkah Al-Mukarramah, Kingdom of Saudi Arabia.
[4]These authors contributed equally to this work.

October 30, 2013

Abstract

The complex dynamics of unconventional computing devices like networks of droplets filled with the self-exciting Belousov Zhabotinsky (BZ) reaction can be hard to track and to understand. Corresponding to recurrent neural networks, the flow of excitations in the network is not limited to a single direction in the droplets. Especially when unconventional computing systems are not engineered but evolved through genetic algorithms, the actual process of computation will often be incomprehensible. Several methods from Information Theory like Transfer Entropy, Information Dynamics, and Information Decomposition offer approaches for observing and analyzing computing systems on a higher level and allow for a better understanding of the involved data transferring and manipulation operations. In this work we show how to discretize the spike trains of BZ droplet networks and how to apply mutual information measures on the time series data of both physical implementations as well as on simulations. While the

physical systems we are investigating are built from few droplets, the simulated system under consideration in this paper comprise up to 100 droplets.

1 Introduction

Droplet Computers

In the scope of the "Artificial Wet Neuronal Networks from Compartmentalized Excitable Chemical Media" (NEUNEU) project, we are constructing and characterizing droplets of the aqueous **Belousov-Zhabotinsky (BZ) medium** (Zaikin and Zhabotinsky, 1970; Noyes et al., 1972; Adamatzky, 2001) coated with a lipid layer and swimming in hydrophobic phase (Aghdaei et al., 2008; Szymanski et al., 2011a). In the oscillatory regime, waves of chemical activity spontaneously appear in droplets with a period depending mainly on the concentrations of reagents. In a single BZ droplet, only self-excitations are possible, yet for the system composed of two or more coupled droplets, the **waves can propagate** from one droplet to another. Such external wave triggering can occur only under certain conditions.

Just after excitation, the concentration of the activator of BZ reaction drops (Gorecki et al., 2011), leaving a slowly decaying repressor concentration, constituting the **refractory state** of the medium. Due to the high level of repressor, a chemical wave from neighboring droplet cannot excite the medium and thus no further wave propagation occurs. However, if the time from the last oscillation is sufficiently long, then **excitable state** begins *i.e.* the concentration of the repressor crosses a threshold level below which an incoming, external wave propagates onwards in form of a directional wave, starting at the connection point of two droplets. Even without external triggering, after the characteristic self-excitation time, the amount of the repressor can fall so low that the droplet **self-excites** spontaneously.

Using these interactions between droplets, classical boolean gate logic can be constructed in experiment and simulation (Adamatzky, 2002; Holley et al., 2011a,b), but also non-boolean, e.g. graph-theory based (Adamatzky et al., 2011) applications are being researched into under the general context of unconventional computing (Adamatzky, 2001; Stepney, 2012; Banda et al., 2013).

While the analogy of the excitation waves to neural spikes inspired the project, we will also try to resort to established techniques of analysis known from the neurosciences (Borst and Theunissen, 1999; Brown et al., 2004; Quiroga and Panzeri, 2009; Wibral et al., 2011) and other sciences involving complex networks, e.g. atmosphere chemistry (Solé and Munteanu, 2004),

ecosystems Sugihara et al. (2012) or biological signaling networks (Pahle et al., 2008) to understand the reason for their computational efficiency and their modes of operation. From another perspective, any innovation on understanding either of these systems might also be applied in the other complex networks related domains.

Challenges

Typically the dynamics of such a possibly recurrent network with a vast amount of interconnected components will be quite rich and complex (Maass et al., 2002; Dittrich, 2005). This typically means, that our common, intuitive, modular, engineering perspective of the system will not be successful any more (Zauner, 2005; Stepney, 2012).

For engineered or evolved systems' or liquid state machines, their functions are usually specified from the outside. In biological systems, a network's function is not necessarily known although we assume it has some function. But for both types of systems we are interested in how the systems perform this function, which elements interact in which way to perform the task. Hence we require a set of perspectives, of filters to view these complex systems with that show and highlight different aspects of the systems. Dynamical Systems Theory (Jetschke, 1989; Williams and Beer, 2010a) is one of these filters. Another filter might be information theory and information dynamics (Shannon, 1948; Schreiber, 2000; Pereda et al., 2005; Lizier et al., 2008; Williams and Beer, 2010a,b), for identifying the key components of information processing: information transmission, modification and storage. While finding the places in the network where information storage is exploited to produce results is certainly of key importance, this concept is not in the scope of this paper. Instead, we focus on information transmission and information modification here.

One further problem of unknown dynamic systems is to fix the symbol encoding when the systems should be used for computation: Different kinds of symbol encodings might be more or less useful for information modification, storage and transmission operations in a particular system (Escuela et al., 2013; Gorecki et al., 2013). For example in case of boolean operations in networks of BZ droplets, it sounds natural to assign a high spike frequency to the symbol '1' and a low spike frequency to the symbol '0'. But a different encoding that might exploit more subtle differences in spike timing, e.g. the time delay between two neighboring droplets, or the activity patterns of a whole set of droplets might prove more useful in certain systems. Nonetheless information theory offers such an approach by abstracting away the particular encoding.

Operational Modes of Droplet Systems

To monitor the flow of information in a droplet network, different techniques can be applied. But first of all, it seems useful to study different operational modes of how the complex system might be used for computation. We consider the operational mode from the point of view of **interfacing** here: Typically for any computing device, some **input** can be specified and then the **output** is retrieved in a specified manner. This input can either be hard-coded in the design, in the initial state of the network or it has to be supplied to the droplets during their lifetime. In the latter case, a number of inputs for a single calculation might be specified by a time-variant or constant stimulation pattern that corresponds for example to boolean values or to real-valued sensor data. Alternatively, a series of calculations might be carried out by varying the input signal, e.g. like a continuous stream of sensory inputs for a robot that has to adapt to its environment all the time. The input droplets are being stimulated from outside the droplet system, as explained in Section 2.1.

Analogously to the inputs, the output of a single computation can either be interpreted in a **time-variant or constant** manner. When different computations are carried out with varying inputs, an additional difficulty arises how to relate which input to the output at what time interval. For example, when an input is communicated to the network in the interval $[t_1, t_2]$, in which interval $[t_3, t_4]$ can the result of the computation be read out? Here, some further mechanism, for example an external clock signal, would be required.

In the simplest case, the simulation or experiment is just observed **undisturbed**, so that only some droplets self-excite and drive the activity of the system. This might be useful, when some parts of the network should be working independent from the input, e.g. as independent signal generators, or as a memory from earlier stimulation.

In this paper nonetheless, we will consider only a single computation per experiment with either (i) a **constant stimulation** pattern as input for the functional analysis, or (ii) a **random spike pattern** for the connectivity analysis, such that we can follow this pattern through the network and study which droplets influence which others.

Overview on this Work

In this work, we show how to analyze an experimental five droplet system as well as simulated droplet systems in the order of magnitude of 100 droplets by following the information flow. That is, on the one hand the information that

is directly **transmitted** from one droplet to droplet by looking at the **time delayed mutual information** between spike patters in both droplets. On the other hand, we can investigate the mutual information between spike patterns in particular droplets and **external values** like specific input classes, their combinations as well as expected outputs of a computation.

In particular with the latter approach, we show how to highlight the **synergy** between different inputs with the mutual information to the expected output of a computation. Typically some positions in the droplet network start showing more information about the output than all their neighbors that supply this droplet with signals. In this case, information is combined and the synergy of the sources is exploited for computation.

2 Methods

In the following, we will show how the video data from experimental observations as well as simulation records can be analyzed with the same information theory based analysis method. Our basic assumption here is, that all the useful information of the droplet activity is found in their spike times, *i.e.* the amplitude of the spike and the behavior of the chemical medium between the spikes is irrelevant and abstracted away. Thus we extract the spike times from the video data of chemical experiments and, analogously, remove all extra information that is available from simulation experiments except for the spike times.

To begin with we will describe our chemical experimentation setup in the next Section, then our simulation of droplets and then the information theory based analysis method.

2.1 Experimental Droplet System

In the experiments with BZ droplets we used commercially available analytical grade reagents without further purification. The solution of BZ reagents contained the following concentrations of BZ components: 0.3 M sulfuric acid (H_2SO_4), 0.375 M sodium bromate ($NaBrO_3$), 0.125 M malonic acid ($CH_2(COOH)_2$) and 0.04 M potassium bromide (KBr). In the experiment we used a mixture of catalysts. The bathoferroin ($[Fe(batho)_3]^{2+}$), which concentration was 0.0015M played the major role. In order to make the medium photosensitive a small amount of ruthenium (Ru(bpy)3Cl2) (0.00021M) was added.

Bathoferroin tris(1,10-bathophenanthrolinedisulfonic acid) is a redox indicator, red in the reduced state and green when oxidized. The waves of oxi-

dized form, spreading in the system correspond to high concentration of the activator and can be traced optically. Moreover the catalyst interacts with lipids on the droplet boundary (Szymanski et al., 2013) and changes the interfacial tension that can enhance the communication between droplets. The other catalyst (Tris(bipyridine)ruthenium(II) dichloride) makes the reaction sensitive to blue light ($\lambda \sim 460$nm). Illumination of the medium leads to production of bromide ions that inhibit the reaction and thus we observe no oscillations in the strongly illuminated area (Jinguji et al., 1992). Illumination with low light intensity increases the period of oscillations.

The experiments were carried out in a Petri dish (50 mm diameter), inclined at a small angle to the horizontal. Solution of a phospholipid L-α-phosphatidylcholine (Soy-20%,Avanti Polar Lipids, Inc.) in decane, prepared by dissolving 0.25 g of lipids in 50 ml of decane, constituted environment for compartmentalised BZ medium.

In all experiments we considered a linear chain of five droplets surrounded by the organic phase. All droplets were identical and they contained (1.4 μl) of the solution. We pipetted the droplets into the dish, where driven by the gravity force they arranged into a linear array in a lower positioned part of the dish. In such a configuration stable connections between them can be maintained on the time span of the experiment, allowing for propagation of pulses via the lipid bilayer. All experiments were performed at 25 °C and the medium was not directly thermostatted.

We controlled oscillations in the droplets by means of high power, blue LEDs (HUEY JANN ELECTRONIC, HPE8B-48K5BF, 5W) connected to a PC through an electronic circuit. Plastic optical fibers (1.5 mm diameter) attached to the diodes allowed to illuminate each droplet individually. The light intensity was adapted during the experiments to obtain required frequency of oscillations for the droplets. The exposure time of each droplet was controlled with 1 ms time resolution.

Light emitting fiber tips were positioned centrally below corresponding droplets to limit amount of light transferred to the surrounding. The experimental system is drawn schematically in Figure 1.

We recorded the time evolution of the system using a digital video camera (Sony HDR-XR550VE) with attached magnifying lens Raynox-505. The video was captured with the resolution of 1440 $\times$ 1080 pixels and frequency of 50 frames per second (fps) and cut into a series of frames. ImageJ software was applied to acquire and process the obtained sequences of images.

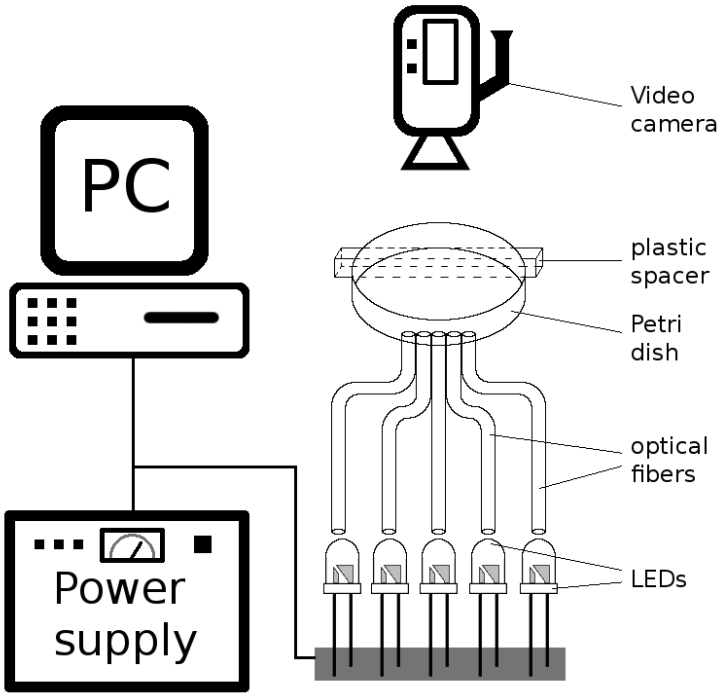

Figure 1: The experimental Setup. PC controlled diodes emit blue light (λ=462 nm), transferred to each droplets separately through optical fibers. The illumination is used to slow down the BZ oscillation in the droplets up to the point where no oscillation occurs. Furthermore, the illumination can be used to set the oscillation phase of droplets and thus also to synchronize multiple droplets.

2.2 Simulated Droplet System

For the *in silico* studies of droplet systems, we used the stochastic, continuous time, discrete event simulation system described in (Gruenert et al., 2013). In this approach, the behavior of the chemical droplets is structured into the three phases denoted the *excited*, the *refractory* and the *responsive* phase. Only in the very short *excited* phase, a droplet can influence its neighbor if that is in the *responsive* phase. A *signal propagation delay* is included to account for the speed of the BZ wave expansion.

The **normal droplets** d_{Norm} in our simulation stayed excited for one second, were refractory for five seconds and then self-excited after 10 seconds if not externally triggered. The signal propagation delay from one droplet to the next was one second. For each of these values, a normal distributed noise term of the standard deviation 0.05 s is added for each event, such that the simulation becomes non-deterministic. Apart from the normal droplets as described above, we used a slightly faster oscillating droplet d_{Fast} with 0.8 times the original period, a slightly slower oscillating droplet d_{Slow} with 1.25 times the original period and a less excitable droplet d_{LowEx} that requires two concurrent excitations at its neighbors to be triggered into an excitation.

When considering not only a single droplet but a complex and **interacting system of droplets**, we will refer to individual droplets as d_i, and to the whole droplet system $D = (d_1, d_2, ..., d_w)$. Because a **two-dimensional structure** is more probably to be reproduced in laboratory experimental setups, we will typically use planar graph structures for the droplets networks here. In this paper, we will typically use u by v droplet arrays N with $u \cdot v = w$ fields: Each field of the array can then either be left empty or contain a different droplet type of a different chemical composition - resulting in slower or faster oscillation behavior or in less excitability. Also, we facilitate inputs to the system by stimulating some of the droplets d_{In0}, d_{In1}, etc. externally via the inhibitive LED illumination, mentioned in Section 2.1.

$$N = \begin{pmatrix} d_{1,1} & d_{1,2} & \cdots & d_{1,v} \\ d_{2,1} & d_{2,2} & \cdots & d_{2,v} \\ \vdots & \vdots & \ddots & \vdots \\ d_{u,1} & d_{u,2} & \cdots & d_{u,v} \end{pmatrix}$$

$$d_{i,j} \in \{\varnothing, d_{Norm}, d_{LowEx}, d_{Slow}, d_{Fast}, d_{In0}, d_{In1}, d_{Out0}\}$$

Then typically, vertically and horizontally adjacent droplets will be able to **interact** with one another while diagonally or more distant droplets are considered to be unconnected (even though they might interact via other droplets). In simulation, nonetheless, other non-planar connectivities can be explored.

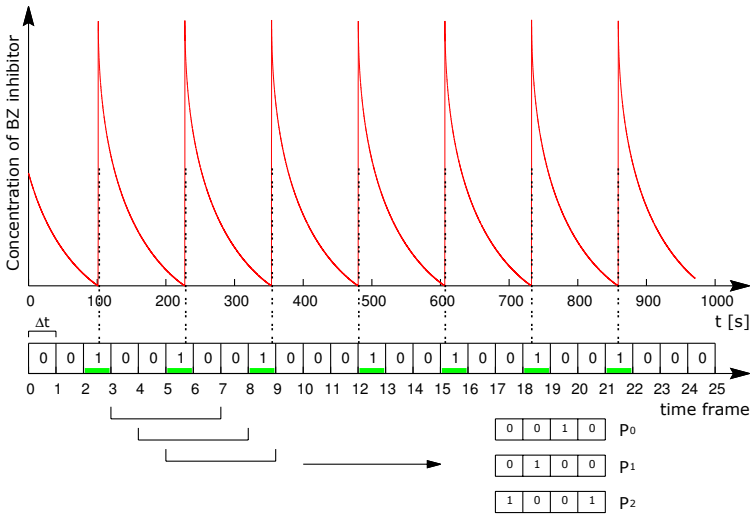

Figure 2: Discretization and extraction of discrete spike patterns from an exemplary spike train using the frame size $\Delta t = 40$s and pattern length $l = 4$.

2.3 Information Theoretic Approach

Symbol Representation

Our basic assumption for measuring the droplet network information transmission is that all information on the dynamics of the droplet system D is present in the **sequence of spike times**. It does not matter whether considering a chemical system observed by video or a simulated droplet system (see Sections 2.1 and 2.2). *I.e.* a given droplet system D's dynamics are sufficiently represented by the set of times $T_{s_d} = \{t_1, t_2, ..., t_n\}$ for each droplet $d \in D$ in the system when it becomes excited. We assume that, in contrast, the amplitude or the exact shape of the excitations can be neglected.

For the measurement of information, we partition the continuous-timed spike train data into discrete symbols (Strong et al., 1998). Let us select the discretization length Δt and define a series of $m = \lceil t_n/\Delta t \rceil$ time intervals $I_1, I_2, ..., I_m$. Here the interval I_j is defined between the times $(j-1)\cdot\Delta t$ and $j \cdot \Delta t$, where $j = 0, 1, ..., m$. Now we convert the **continuous spike train** T_{s_d} of droplet d into a binary sequence of either zeroes or ones, resulting in the **discretized spike train** $S_d \in \mathcal{S} = \{0, 1\}^m$. Any time frame I_i that contains at least one spike at time $t_j \in T_s$ is set to value 1 while all other frames are set to 0. Reformulated as sequence of bits, a single spike train $S_d \in \mathcal{S}$ is now written as $S_d = (a_{I_1}, a_{I_2}, ..., a_{I_m})$.

$$I_j = [\ (j-1)\Delta t\ ,\ j\Delta t\ [$$

$$m = \lceil t_n/\Delta t \rceil\ ,\ a_{I_i} \in \{0,1\}$$

$$a_{I_i} = \begin{cases} 1, & \text{if } \exists\ t_j \in T_s \text{ such that } t_j \in I_i \\ 0, & \text{if otherwise} \end{cases}$$

From the completely discretized spike train S_d of a single droplet d, consisting of m frames for the whole experiment, we use a sliding window of length $l << m$, resulting in a set of $m - l + 1$ **discrete spike patterns** $P_1, P_2, ..., P_{m-l+1}$. Spike pattern $P_i \in \mathcal{P} = \{0,1\}^l$ is defined for the time intervals $I_i, I_{i+1}, ..., I_{i+l-1}$.

So far, spike trains and patterns are defined for a single droplet d only. But because the dynamics can be influenced not only by a single droplet but by the **interaction of many droplets** as well, e.g. population coding, we can also consider spike patterns that are built by observing many droplets at the same time.This expands the discretized representation of patterns $P_i \in \mathcal{P} = \{0,1\}^l$ to become a two dimensional array instead. By adding another dimension for the droplet, the set of all patterns becomes $P_i \in \mathcal{P} = \{0,1\}^{k \cdot l}$, where k is the number of aggregated droplets and l is the length of the sliding window. Nonetheless, in the examples shown in this paper, we will only use spike trains and spike patterns for single droplets.

For our information theoretic approach, we consider the spike patterns P_i to be the basic symbols. That means we will **estimate the probability distribution** over all the patterns appearing in experiment or simulation as well as the joint distributions of the patterns together with different external inputs or expected outputs of the computations. From a recorded or simulated whole spike train we estimate the probability distribution $p(P_i)$ for all possible spike patterns $P_i \in \mathcal{P}$. For the pattern length l and the number of considered droplets k, there are $2^{k \cdot l}$ different patterns. Even though this number seems huge, only a small subset of all possible spike patterns do actually appear. Given that the time discretization Δt is small in comparison to the oscillation period τ of the droplets, most time frames $a_{I_i,d}$ are zero.

Spike Train Entropy

We can now measure the entropy of a discretized spike train by using the standard **Shannon entropy formulation** (Shannon, 1948) over the distribution of spike patterns found in the spike train:

$$H(\mathcal{P}) = -\sum_{P_i \in \mathcal{P}} p(P_i)\ \log_2\ p(P_i)$$

For a given discretization raster Δt and for a pattern length l, this measures the entropy of the spike patterns. Clearly, this value does not only depend on the complexity of the spike train, but also on the chosen (Dimitrov and Miller, 2000) length of the spike pattern l, on the discretization interval Δt and on the number of simultaneously observed droplets k. So for example, when reducing the raster size Δt or when increasing the pattern length l the Entropy of the observed patterns will increase due to the higher number of possible patterns.

As we discussed before, sometimes the information, for example from an intermediate computation, might not be found in exactly one droplet but can be found "de-localized" over two or more droplets. This possibility is already captured by our definition of the spike patterns that can be built from single as well as from multiple spike trains.

Spike Train Mutual Information

As mutual information is widely used as an indicator for correlation, it also qualifies as a natural candidate for **finding dependencies** between two droplets or between two groups of droplets in a network. The common mutual information formulation

$$I(\mathcal{P}_a : \mathcal{P}_b) = H(\mathcal{P}_a) + H(\mathcal{P}_b) - H(\mathcal{P}_a, \mathcal{P}_b)$$

can directly be applied to two different spike pattern distributions $\mathcal{P}_a$ and $\mathcal{P}_b$, where $a, b \subseteq D$ refer to different subsets of droplets in the network D. Typically, a and b will be non overlapping, such that $a \cap b = \emptyset$. Here, the joint entropy $H(\mathcal{P}_a, \mathcal{P}_b)$ refers to the probability distribution of both patterns $P_i \in \mathcal{P}_a$ and $P_j \in \mathcal{P}_b$ happening at the same time.

$$H(\mathcal{P}_a, \mathcal{P}_b) = -\sum_{P_i \in \mathcal{P}_a} \sum_{P_j \in \mathcal{P}_b} p(P_i, P_j)\ \log_2\ p(P_i, P_j)$$

The symmetric values $I(\mathcal{P}_a : \mathcal{P}_b)$ gives a the average number of bits that are known about a spike pattern from $\mathcal{P}_a$ by knowing the spike pattern from $\mathcal{P}_b$ or vice versa.

This measure should be independent from a particular **symbol encoding scheme**. For example, a strange encoding scheme might be to store the message in the exact delay between one spike and the third-next spike, while the two intermediate spikes are of no importance. Given that the important

features of a spike train are visible on the resolution Δt of the discretization and fit in the pattern length $l \cdot \Delta t$, the mutual information between the spike trains can be used also to measure complex and non-linear dependencies.

Still, when measuring the dependency between any two droplets, the general problem arises to **distinguish** between correlation that is generated because droplets are independently swinging with a fixed phase delay but without influencing each other, and on the other side, those droplets that are correlated because they are **actively influencing each others dynamics**. If they are unconnected, we might still measure high mutual information, e.g. when both droplets are oscillating with the same frequency or with integer valued multiples of the frequencies.

Transfer Entropy (Schreiber, 2000; Staniek and Lehnertz, 2008; Wibral et al., 2011) resolves this problem by taking into account the past of a possibly influenced variable. Hence, transfer entropy is only measured when a variable's own past does not suffice to explain its future behavior. Furthermore, using transfer entropy, it becomes possible to determine the **direction of the influence** because it is not a symmetrical value as mutual information. While theoretically sound, this approach did not work well in the context of droplet computers for us so far, most probably due to the problem of sampling sufficiently long history data. More advanced sampling techniques might help to produce better estimates of the correct pattern probability distribution, though (Panzeri and Treves, 1996; Strong et al., 1998; Roulston, 1999; Nemenman et al., 2004). Furthermore, as mentioned in (Wibral et al., 2011), optimal auto-prediction, *i.e.* the prediction of a nodes state from its past, is a prerequisite for inferring the causal relationship. This auto-prediction is in particular difficult, when the natural oscillation frequency of the droplets is constantly changing in chemical experiments.

Another simple approach is to combine measurements of many experiments with **different initial conditions**, such that a fixed phase shift dependency is broken. With this approach, we can distinguish droplets that are actually influencing each other from those that are only coupled by a particular initial phase. But especially in the case of chemical laboratory experiments, some of them are hardly repeatable. Also, the mutual information is still a symmetric value, such that we cannot determine the direction of the influence. For these reasons we used time delayed mutual information as explained in the next Section.

Time Delayed Mutual Information

Excitation waves require time to travel from one part of the droplet system to another, so one droplet can not influence another droplet without **time**

delay. In principle, excitation waves can travel in either direction if the direction is not explicitly enforced (Szymanski et al., 2011b). Here we assume that the **signal propagation direction is mostly fixed** for a specific stimulation situation, and thus also the time delay between the spike patterns in a pair of two droplets becomes constant. So we calculate the mutual information between the spike patterns at droplet d_a for all times t and the spike patterns of another droplet d_b at times $t + \tau\Delta t$ for a limited range of τ values by the formula:

$$I^{\tau}_{TD}(\mathcal{P}_a : \mathcal{P}_b) = H(\mathcal{P}_a) + H(\mathcal{P}_b) - H(\mathcal{P}_a(t), \mathcal{P}_b(t + \tau\Delta t))$$

Here, $H(\mathcal{P}_a(t), \mathcal{P}_b(t+\tau\Delta t))$ is the entropy of the joint, but time shifted, spike trains.

Assuming that one droplet is most influencing another droplet at a specific time delay, we use the time delayed mutual information (Fraser and Swinney, 1986; Pereda et al., 2005; Jin et al., 2010) to estimate the mutual information between two droplets and their time delay at the same time. At a time delay τ', when the time delayed mutual information is maximal, the interaction between the droplets should be strongest. Formally, we note this assumption as:

$$\begin{aligned} I(\mathcal{P}_a : \mathcal{P}_b) &= \max_{\tau} \quad I^{\tau}_{TD}(\mathcal{P}_a : \mathcal{P}_b) \\ \tau' &= \operatorname{argmax}_{\tau} \quad I^{\tau}_{TD}(\mathcal{P}_a : \mathcal{P}_b) \end{aligned}$$

This measurement also reveals the **effective signal speed** in the network that might differ from the chemical wave propagation speed. For example, when starting two wave patterns at both ends of a linear chain of droplets, it will take some time until the wave with the higher frequency can take over the control of the whole system: But the front where both waves collide will move slower to the end of the slower pattern generator than the individual waves would travel.

Information Between Spike Trains and External Values

Instead of correlating the behavior of a specific droplet to another droplet's spike pattern, we can also compare it to **external values** such as the **input class** or the **expected output** class. We use the term input/output class here to distinguish the symbol from its representation as a specific spike pattern: In this case we calculate the mutual information of a spike pattern with the abstract input/output symbol only. For example, when considering a pattern recognition task where low, average and high chemical concentrations are sensed, there is no necessity of encoding a low chemical concentration in a low frequency spike signal. Instead, the low concentration could be encoded

NOR	i_1	i_2	o_1
case_1	0	0	1
case_2	0	1	0
case_3	1	0	0
case_4	1	1	0

Table 1: Input cases/output symbols for the four input cases of the NOR function.

as high frequency or more complex spike patterns could be used, maybe even keeping the average spike frequency constant (Escuela et al., 2013).

A problem definition for a function with a finite number of input cases $i \in \{1, 2, .., p\}$, can be given in the form of a table, where the expected output values are listed for each input case i. An example is shown in Table 1 for the NOR function. Here we denote each input or output row j of the table as i/o-channel. Not distinguishing between **input and expected output symbols** here, We might be interested in the mutual information between **any combination** of them and the spike patterns found in particular droplets. Followingly, we use the symbol γ for a combination of rows from the function definition table. For the function with two inputs and one output as defined in Table 1, γ is a subset of the inputs i_1,i_2 and the expected output o_1: $\gamma \subseteq \{i_1, i_2, o_1\}$. Not distinguishing between inputs and expected outputs is then useful because we can use the same formalism to analyze the mutual information of spike trains with different input channels, output channels or combinations thereof.

For any droplet a in the network, the mutual information with the combination of i/o channels γ is then calculated under the assumption that any input case i has the same probability:

$$I(\mathcal{P}_a : \gamma) = H(\mathcal{P}_a) + H(\gamma) - H(\mathcal{P}_a(t), \gamma)$$

This implies, that the droplet system is **observed or simulated for all the input cases** i. The joint entropy between the input/output channel combination γ and a spike pattern $P \in \mathcal{P}_a$ can for example be generated by concatenating the input/output symbols contained in γ for each case i to the spike pattern P that it was generated with.

Studying Table 2, we can see, that the mutual information between an input channel and the output of the computation can either vanish completely, for example in the case of the XOR function, or stay completely intact as in the case of the NOT function. Furthermore, in the case of the OR or NOR functions, even though there is information about the output present in each

	$H(i_1)$	$H(i_1, i_2)$	$H(o_1)$	$H(i_1, o_1)$	$I(i_1 : o_1)$
IDENTITY	1	-	1	1	1
NOT	1	-	1	1	1
AND	1	2	0.81	1.5	0.31
OR	1	2	0.81	1.5	0.31
NOR	1	2	0.81	1.5	0.31
XOR	1	2	1.0	2	0

Table 2: Information theoretic properties of typical deterministic boolean functions: Some further properties are $H(i_1) = H(i_2)$ and $I(i_1 : i_2) = 0$ by definition for two input functions with equally distributed and independent boolean input cases. $H(i_1, i_2) = H(i_1, i_2, o_1)$, because all the information of the output is already present in the input. This also implies $I(i_1, i_2 : o_1) = H(o_1)$, if the output is at all dependent of the input.

of the single inputs already, this information does not sum up to the entropy in the output. Hence, a **synergy between the input channels** is exploited for computing the output by combining both inputs. In the extreme example of the XOR function this becomes obvious: It is not possible to make any judgment about the output, if only either of the inputs is known.

3 Results

3.1 Information Flow in Experimental Systems

The experiment discussed below was conducted as described in Section 2.1. From the total recorded time evolution of five droplets of length 4505 s, we considered the data from the time interval [1585 s, 4505 s]. The initial part of the experiment contained the setup procedure and thus early data were neglected.

The frames from the considered interval were extracted at the rate one frame per second. This produced a video stream of 2920 video frames. To observe the time evolution of oscillations in the droplets d_1 till d_5, arranged in a linear chain as shown in Figure 3a, we cut the series of frames along the bright line and obtained the space-time plot presented in Figure 3b.

Bright, periodic stripes correspond to the high level of the oxidized form of bathoferroin and they mark the moments of time at which the excitations occurred. We identified 28 excitations for the droplets d_1 and d_4, 27 excitations for d_2 and d_3 and 29 excitations for d_5. The minimum observed oscillation period was 63 seconds, ranging up to 190 seconds when the medium

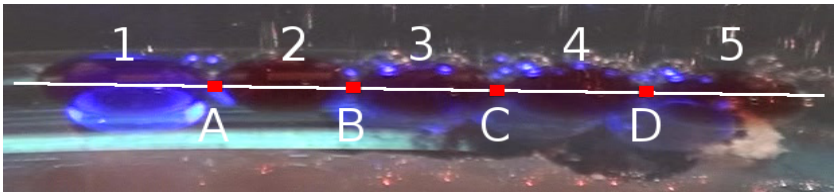

(a) Snapshot of the experimental 5 droplet system.

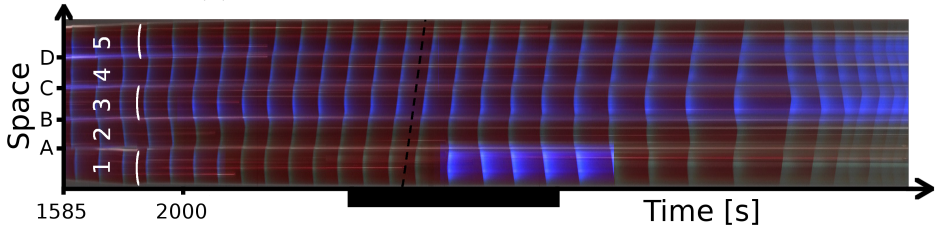

(b) Space-time plot of the white axis displayed in panel (a).

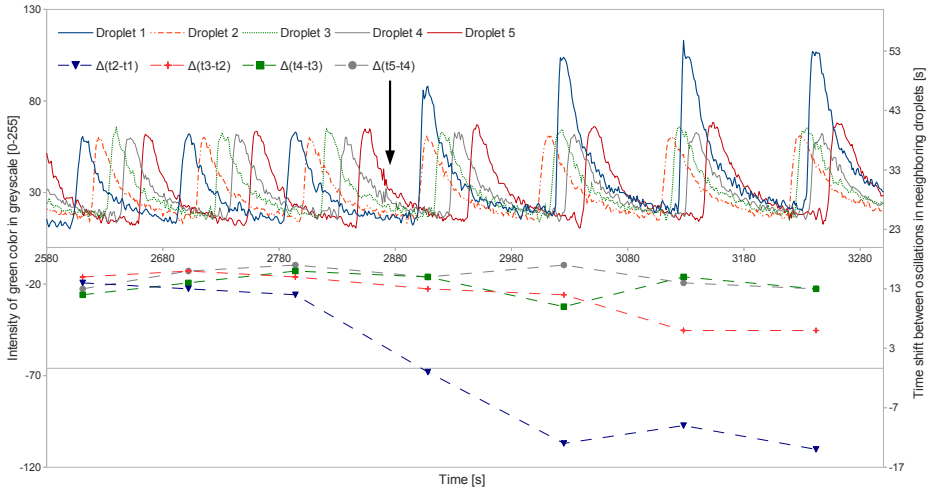

(c) Oscillation diagram.

Figure 3: (a) A snapshot from time evolution of five droplet system. (b) Space-time plot obtained by cutting the series of frames along the bright line drawn in Figure (a). White, slightly curved lines schematically represent the shape of wavefront, characteristic for self-excitations. The dashed, black line indicates the part of the experiment at which the activation sequence of excitations 1→2→3→4→5 was observed. The black rectangle at the time axis marks the part of experimental results corresponding to the time series in Figure (c). (c) Intensity of green color at the geometrical centers of the droplets as a function of time. The distance between the maxima in a selected droplet determines the period of oscillations, whereas for two different droplets indicates time shift between forced oscillations. The arrow marks the moment of time (t=2862 s) at which we started to illuminate droplet (1). The illumination was ceased at t=3484 s.

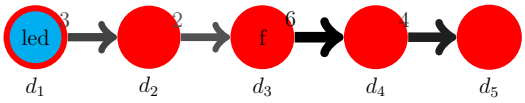

Figure 4: Schematic illustration of the five droplet network from Figure 3a and the measurement of time delayed mutual information. The three droplets d_3, d_4 and d_5 are slightly slowed down by blue illumination. Droplet d_1 is controlled by the LED. Droplet d_2 is probably also influenced by the LED of droplet d_1. Hence droplets d_1 and d_2 mostly control the remaining part of the droplet system. The arrows indicate that we measured a time delayed mutual information with the ideal delay in frames displayed at the base of each arrow. We measured the strongest time delayed mutual information between droplets d_3 and d_4 with a time delay of 6 frames, corresponding to $6 \cdot \Delta t = 18s$.

was nearly depleted.

In the initial part of the experiment the droplets (1), (3) and (5) oscillate spontaneously as marked schematically with the white, curved lines. Initiation center of the chemical wave for the self-excitations is located typically close to the geometrical center of the droplet and then the wave travels outwards. When it reaches the connection with a neighboring droplet, that is in the excitable state then the activation occurs. In that case we observe a directional wave visible as inclined stripes on the space-time plot, with the initiation center at the connection point.

During the time-span of the experiment we illuminated droplets d_3, d_4 and d_5 with a low light intensity. As the result, the non-illuminated droplets d_1 and d_2 oscillated fastest. Approximately at experimental time $t = 2800s$, the waves originating from droplet d_1 spread out through the complete droplet chain, effectively controlling the oscillations of the remaining droplets. Then, at time $t = 2905s$, we turned on the illumination of droplet d_1, leading to slower oscillations in that droplet. This illumination until time $t = 3506$ changed the dynamics in the investigated network: Droplet d_3 started taking over controlling the oscillations of the network till the end of the illumination but was superseded by droplet d_1 afterwards. We use this changing dynamics as a source of entropy in the droplet chain and follow the information flow from the illuminated droplets by means of time delayed mutual information.

For each pair of adjacent droplets, we calculated the time-delayed mutual information, resulting in the directions and time delays displayed in Figure 4. For the pattern length $l = 30$ frames and frame length $\Delta t = 3s$ we obtained entropy values of about 4.8 bits per droplet and maximal mutual values between 1.98 (d_2 to d_3) and 2.87 (d_3 to d_4) bits. These measures support

the observation that information is transferred from the random source, the illuminated droplet d_1, to the droplets on the right.

Nonetheless, about 30 observed excitations do hardly suffice to build a probability distribution of spike patterns, in particular, when the oscillation times are constantly and continuously changing as the medium is aging in this example. Since the medium is changing in a similar way for all droplets in the system, a correlation between each droplet's behavior might be measured. But because this correlation should be similar for all delay values, the maximum of the information over the different time delay values should still be a useful indicator for the actual interaction.

3.2 Hand-designed Linear Classifier Network

Because real droplet experiments cover a small number of oscillations from the point of view of information theory, further experiments are carried out in **simulation**. The future use of microfluidic devices will hopefully improve the reproducibility of the experiments, though. First we will introduce and analyze a hand-designed linear classifier network design as well as an evolved binary NOR gate. Then we will show how the information flow measures can support studying the function of network components' functions my modifications.

A simple linear classifying network was hand-built in simulation for classifying samples from the *Proben1* (Prechelt, 1994) data set. Each data sample from the *cancer* subset is a 10 elements vector where the first 9 values, $\{i_1, i_2, ..., i_9\}$ are from the set of 9 discrete values $\{0.1, 0.2, ..., 0.9, 1.0\}$ while the last value is the binary output class, either *benign* or *malign*. Of the 699 samples, 458 are from the *benign* class, while 241 are for the *malign* case. This results in an output class entropy of ca. 0.93 bits. For the same data set, we already presented the evolution of a generative network description (Diem et al., 2012). But in contrast here, we hand-designed this network with the rationale of selecting out of the nine input signals those three with the jointly **highest mutual information to the expected output class**, *i.e.* the inputs i_1, i_2 and i_6 combined, jointly having a mutual information to the output class of ca. 0.83 bits. First we will combine the two inputs with the highest joint mutual information, $i2$ and i_6, and then combining the result with the input i_1. These three inputs are fed into the droplet network as analogue, rate coded signals, where the value 0.1 corresponds to the lowest spike frequency, very close to self-excitation, while 0.9 corresponds to a very high spike frequency, very close to the highest possible spike rate.

Because, according to Figure 5a, most of the samples of class 1 are in one sector of the input values, a **linear classification** as symbolized by the black

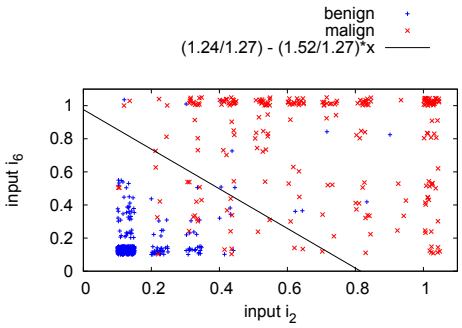

(a) Scatterplot of the input variables i_2 and i_6 of the *Proben1*, *cancer* data set. To simplify the visualization, a uniform random number between 0 and 0.05 is added to the discrete input coordinates i_2 and i_6.

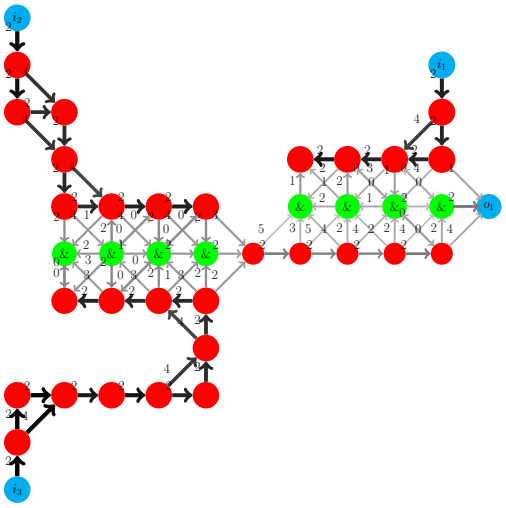

(b) Droplet network design for classification and information flow with random stimulation at the input nodes i_1, i_2 and i_6. Different colors indicate different droplet types.

Figure 5: Test cases (a) and hand-designed droplet network (b) for classification of the *Proben1*, *cancer* data sat. Spike train discretization with $\Delta t = 0.5s$ and a window size of 45 frames. The maximum entropy per droplet was 9.88 bits, the minimum 5.33 bits. Maximum time-delayed mutual information between 1.49 and 8.78 bits. Differently colored circles represents different droplet types, where the red circles represent the standard droplet model as described in Section 2.2. Green droplets marked with the '&' symbol are of lower excitability and require two synchronous excitations in adjacent droplets to trigger an excitation.

line allows a correct classification level of 94%. The droplet network design shown in Figure 5b performs this task when used with an ideal, external threshold function to a similar level of typically more than 90%.

When applying random stimulation at all three input nodes, we can nicely follow the propagation of the **time delayed mutual information**, droplet by droplet, from the inputs i_1, i_2 and i_3 to the central less excitable nodes and towards the output node o_1 in Figure 5b.

Analogously, when observing the mutual information with the **external input symbols**, we can follow the input information of each channel individually in Figure 6. Also, we see that the information about the input symbols is decaying on its way to the central rows of less excitable droplets (green). Another aspect of these plots is, that, for example in Figure 6a,

the information about i_1 is not zero at the other input nodes i_2 and i_3. The reason here is, that there is already mutual information in the input symbols in the data set.

Surprisingly, when considering Figure 6d, the mutual information between the spike patterns and the **expected output** declines when moving from either input along the droplet network towards the output droplet. That means, while a lot of information about the correct outcome of an experiment is present in the inputs initially, this information seems to be lost throughout the network. Nonetheless, the classification using a simple threshold function at the output works relatively well. The reason for this apparent loss of the information about the result towards the end of the computation lies in the considered time frame of the spike patterns: The threshold function works an the averaged spike frequency over the whole experiment of 4000 s while our spike patterns only covered 22.5 seconds. But it is difficult to estimate the probability distribution of all possible spike patterns for patterns larger than 50 frames in this case. For estimating an average of the spike frequency over 200 seconds, 400 frames would be necessary at a frame length of $\Delta t = 0.5$ s. To measure the mutual information with the 200 seconds averaged spike frequency, we discretize the spike range of appearing spike frequencies into 10 different classes and build the probability distribution on the abundance of these classes instead. When using this **average spike rate** as discretization scheme instead for the mutual information measurement as shown in Figure 7, we observe an increase of the mutual information with the expected output class towards the output droplets.

3.3 Information Flow in an Evolved NOR Gate

After using evolution to design boolean logic gates from droplets, information flow analysis can be used to understanding its function. In this example, a **NOR gate was evolved** in simulation, forming the design shown in Figure 8a. Using trivial rate coding, the NOR function implies that for a high frequency stimulation on either or both input channels, a low frequency should be found on the output droplet, while a low frequency on both input channels should lead to a high frequency output. From the time delayed mutual information diagram, shown in Figure 8a, the network's mode of operation can hardly be deduced. When observing the information flow in dependence of the inputs and in comparison to the expected output (cf. Figures 8b,8c, and 8d), it becomes obvious that a very good output of the computation is accumulated at the the top left $\&_1$-droplet, very close to the input i_1. Furthermore, wherever the actual computation takes place, the result has to be transferred to the output droplet o_1. Along the way, some of the informa-

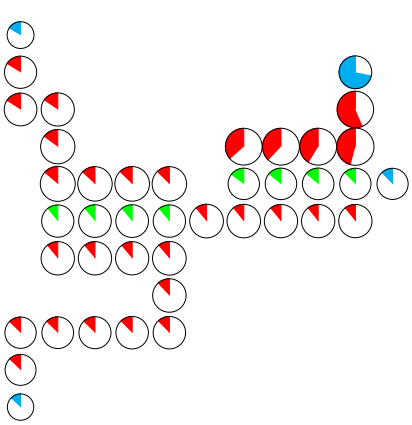

(a) Mutual information with input i_1.

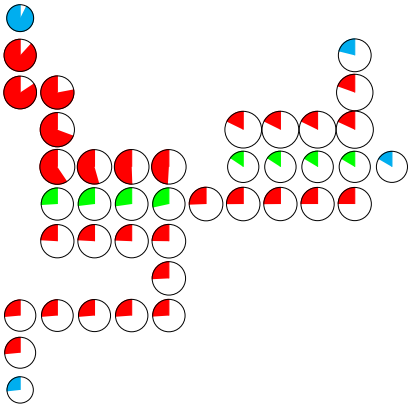

(b) Mutual information with input i_2.

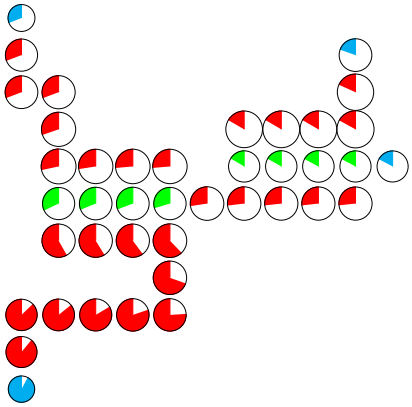

(c) Mutual information with input i_6.

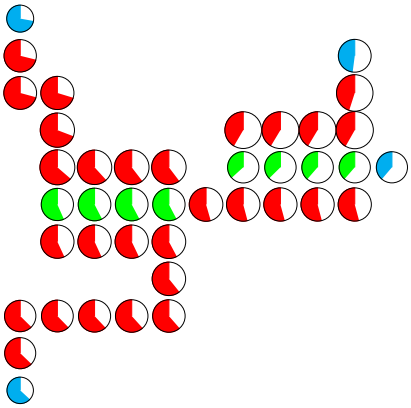

(d) Mutual information with expected output o_1.

Figure 6: Mutual information between each droplet's spike train and the external input or expected output symbols. Spike train discretization with $\Delta t = 0.5s$ and a window size of 45 frames. We measured spike pattern entropies per droplet between 5.4 and 9.7 bits. Entropy of the external inputs i_1, i_2, i_6 and the expected output o_1 were 3.0 bits, 2.3 bits, 2.0 bits and 0.93 bits, respectively. These external entropy values were used as reference for the per-droplet pie charts displayed. The colored fraction of the pie chart corresponds to the mutual information between this droplet's spike train and the external reference symbol, such that a full pie chart would indicate the maximal possible mutual information between the spike patterns and the external input/output. Different colors indicate different droplet types as explained in Figure 5b.

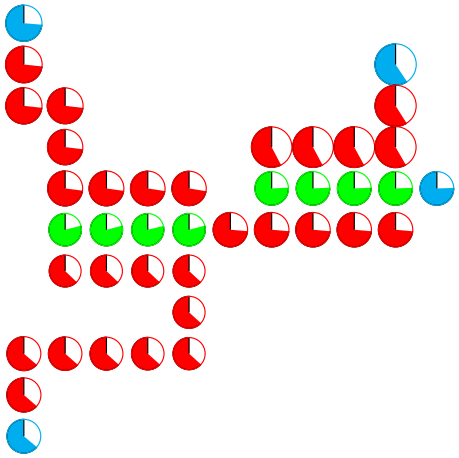

Figure 7: Using a different spike train discretization, the increasing mutual information with the expected output becomes visible. Instead of using the distribution of all possible spike patterns, we only averaged the number of spikes in a window of 200 s and distinguished 10 different bins here. Except for the discretization, this plot in analogy to Figure 6d.

tion may get lost again. When directly tapping the signal from the top left droplet instead, the noise level in the rate coded result of the computation is actually reduced.

This leads to our assumption about the **network function**, that the actual computation, the modification of information both dependently on inputs i_1 and i_2 happens in droplet $\&_1$. The long trail of "full" droplets in Figure 8c on the other hand only transfers the information from input i_2 to the "computing center" $\&_1$, but also relays the result of the computation back to the output droplet o_1. In the next section, we will further investigate this assumption.

3.4 Effect of Manipulating the Information Flow

Mutual information analysis between spike patterns and inputs or expected outputs can also be used to better understand the function of particular droplets in the network by doing **mutation or deletion** experiments. Here we investigate the thesis that the computation of the NOR network is happening in the top left $\&_1$-droplet as implied by the high mutual information to the expected output, shown in Figure 8a.

To investigate this, we first exchange droplet $\&_1$ by a normal droplet. This leads to a globally spread mutual information with the expected output, shown in Figure 9a. But this also leads to an inversion of the spike frequency

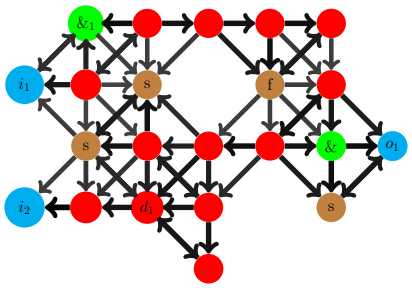

(a) Evolved droplet network as NOR gate and its droplets' interaction diagram.

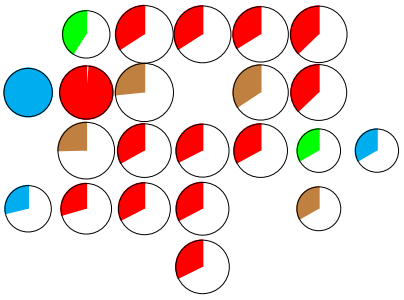

(b) Mutual Information between spike trains and external input symbol i_1.

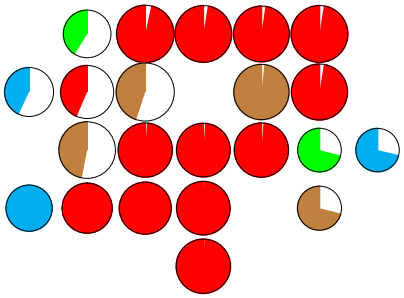

(c) Mutual Information between spike trains and external input symbol i_2.

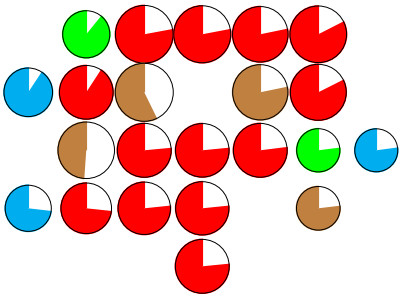

(d) Mutual Information between spike trains and expected output symbol o_1.

Figure 8: This evolutionary designed droplet network is supposed to calculate the binary NOR function. Differently colored circles represents different droplet types, where the red circles represent the standard droplet model as described in Section 2.2. Brown droplets marked with 's' are slightly slower and those marked with 'f' are slightly faster than the red droplets. Green droplets marked with the '&' symbol are of lower excitability and require two synchronous excitations in adjacent droplets to trigger an excitation.
Spike trains are discretized with a frame size $\Delta t = 1s$ and $l = 35$ frames. The displayed sizes of the droplets indicate the entropies of the spike trains which were between 5.4 and 9.5 bits. (a) Arrows indicate the direction of the time delayed mutual information between neighboring droplets. (b-d) Entropies of the external inputs i_1, i_2 and the expexted outputs o_1 were 1 bit, 1 bit and 0.81 bits, respectively. In analogy to Figure 6, these Entropy values were used as reference for the per-droplet pie charts displayed, such that a full pie chart would indicate the maximal possible mutual information between the spike patterns and the external input/output.

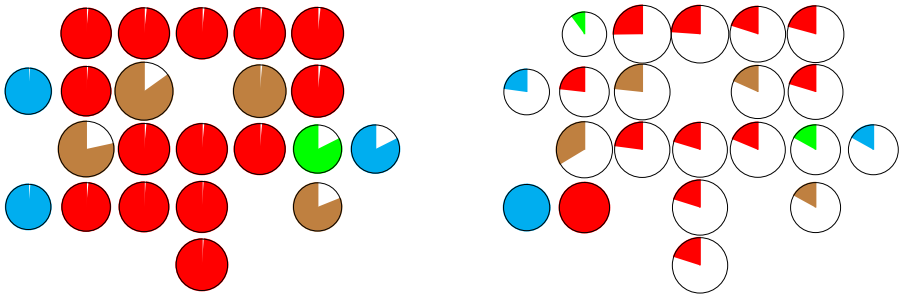

(a) Mutual Information between spike trains and expected output symbol o_1 for modified droplet $\&_1$.

(b) Mutual Information between spike trains and external input symbol i_2 for deleted droplet d_1.

Figure 9: Effect of modificiations on the information flow of the network design from Figure 8a.

for each input case, *i.e.* the whole network acts as an **OR gate instead** of a NOR gate. Note that an OR gate can produce the complete 0.8 bits of mutual information with the expected NOR output, because the inversion of the signal encoding does not destroy information. Nonetheless, building an OR gate from droplets is far simpler than a NOR gate (Escuela et al., 2013). Hence the $\&_1$ droplet is necessary for the correct network function.

In another experiment, we **removed droplet** d_1 from Figure 8a, because it is distant from the possibly important center of computation $\&_1$. Then, the output mutual information is reduced in almost all nodes of the networks. In particular in the top left $\&_1$ droplet, the output mutual information is reduced to almost half its original value. The reason here is probably the perturbed information flow from input i_2 to the computing center $\&_1$ that becomes obvious when comparing Figures 8c and 9a. Because the information from input i_2 does not arrive at the droplet $\&_1$ where it should be combined with input i_1, the **synergy** of the inputs cannot be exploited in the modified network.

4 Discussion

In this work, we presented the measurement of the propagation of information from droplet to droplet in a system of connected, information processing droplet computers.

The principle advantage of the information theory based approach of understanding the droplet systems' work is that we become **independent from a particular symbol encoding scheme** (Strong et al., 1998). In

principle it should be possible to represent any kind of encoding as a spike pattern, given the spike patterns' length l is sufficiently long and the time rasterization Δt is sufficiently small. For example in Section 3.2, we observed a case where the practical pattern length was not sufficiently long to capture the mutual information with the computed output as seen in Figure 6d. Only when we switched to another method of discretizing the spike trains, by taking the average spike frequency over a long time period, we observed the mutual information with the expected output in Figure 7. By deciding for a particular pattern length l, we are measuring the average reduction in uncertainty about either another droplet or external values, when looking at a single pattern sample. Due to limited experiment length (real droplets are depleted after 20 - 100 excitations), due to limited experiment reproducibility and due to limited computational resources, it will not be possible for arbitrary long spike patterns to estimate their probability. When we enlarge the spike pattern length l by one, the number of possible patterns 2^l doubles even though not all spike patterns will actually appear because of comparatively long refractory times. Nonetheless, there are methods (Panzeri and Treves, 1996; Strong et al., 1998; Roulston, 1999; Nemenman et al., 2004) for calculating correction terms for the limited sampling. In this paper though, it was possible to reconstruct the information flow in the experiments and simulations albeit using naive sampling of the appearing patterns.

Another problem of using time-delayed mutual information but also of transfer entropy is the assumption that the **cause and effect relationship**, and thus also the time delay between two droplets, would be constant in a droplet network. This might not always be true, as we see for example in the case of an XOR network (Escuela et al., 2013) that the direction of signal propagation is changing with changing input patterns. Mutual information between spike trains and external symbols should not be affected by this effect so much, because it does not matter what generates the spike patterns in a droplet or set of droplets.

Furthermore, due to the energy consumption of the BZ medium and the non-equilibrium dynamics, its composition as well as its **oscillation dynamics are constantly changing** over the course of the experiment. On the one hand, this complicates the sampling of all possible spike patterns because it might be hard to repeat a particular situation, on the other hand it might produce the "symptoms" of correlations between all the droplets in the system, even though they are not really coupled by wave propagations. But a droplet's past is not sufficient to predict the varying next oscillation pattern, which might lead to an erroneously measured transfer entropy.

Even though we considered only the spike trains of single droplets in the presented examples, the information of an input signal or of intermediate

computations might be **spread over multiple droplets**. In that case, only the combined spike trains of many droplets would reproduce the complete information. Our framework for spike pattern entropy and mutual information is readily suited to capture this kind of information from aggregated droplets, even though it becomes harder to sample the distribution of spike patterns then.

When calculating the time delayed mutual information, as in Figures 4 or 5b, instead of only plotting the time delay implying the maximal mutual information, it might be more useful to plot the complete diagram of **mutual information vs. time delay**. This plot would show if an expressed peak in the mutual information actually exists at a particular time delay. Generally, when calculating the (time delayed) mutual information between spike trains, many times a correlation between **physically disconnected** droplets can be measured. One reason for this effect are similar oscillation periods found in most droplets of the system, such that in a single experiment, once the initial conditions are fixed, one droplet's state can be predicted from another, unconnected droplet. Another reason is, as seen in figure 6, that already the supplied inputs cases might show some correlation.

Considering the Mutual Information of spike trains with external inputs or with expected output values, we have shown that we can identify those droplet that fulfill important functions in the network. But what might be even more important, this measure is in principle independent of the used symbol encoding scheme. This becomes more important when considering the possibility of **mixing different symbol encoding** schemes in a single system. When considering a complex task in a neuronal or droplet system, some **subtasks** will be easier in one encoding scheme than in others. Hence, we might want to mix different encoding types like rate coding or population coding and also vary the assignments between the signals and symbols to optimally exploit the capabilities of the computing medium. Furthermore, for more complex tasks, we might also suspect **possible intermediate results** for the computation. In future works it might also be useful to observe the mutual information between spike pattern distributions and these intermediate results for the desired computation. In this way we might even better follow the course of the computations and gain more insights on how it is achieved.

By following the information flow in unconventional computing systems which are for example built from BZ droplets, we gain a deeper **understanding** of the processes that are actually happening while abstracting away some physical peculiarities and properties of the system. So a very similar kind of analysis should be possible in other non-BZ systems, given a suitable discretization of the used signals. We hope that this kind of analysis

will in future also allow a different concept for **designing, specifying and synthesizing** blueprints of unconventional computing systems, based on information flow. For example, instead of using evolution with an unbiased mutation operator to design droplet systems, we might use an evolution-inspired system that has a **bias on where to apply mutations**, similar to a tinkerer that does not know the effect of his actions but has an idea of where the information flow is impeded.

5 Acknowledgement

The research was supported by the NEUNEU project (248992) sponsored by the European Community within FP7-ICT-2009-4 ICT-4-8.3 - FET Proactive 3: Bio-chemistry-based Information Technology (CHEM-IT) program. The financial support of the Foundation for Polish Science (MPD/2009/1/styp14) to KG is gratefully acknowledged.

References

A. Adamatzky. *Computing in nonlinear media and automata collectives*. IOP Publishing Ltd., Bristol, UK, 2001.

A. Adamatzky. *Collision-based computing*. Springer Verlag, 2002.

A. Adamatzky, B. de Lacy Costello, J. Holley, J. Gorecki, and L. Bull. Vesicle computers: Approximating a voronoi diagram using voronoi automata. *Chaos Solitons and Fractals*, 44:480–489, 2011.

S. Aghdaei, M. Sandison, M. Zagnoni, N. Green, and H. Morgan. Formation of artificial lipid bilayers using droplet dielectrophoresis. *Lab Chip*, 8(10):1617–1620, 2008.

P. Banda, C. Teuscher, and M. R. Lakin. Online learning in a chemical perceptron. *Artificial Life*, 19(2):195–219, 2013.

A. Borst and F. E. Theunissen. Information theory and neural coding. *Nature Neuroscience*, 2(11):947–957, 1999.

E. N. Brown, R. E. Kass, and P. P. Mitra. Multiple neural spike train data analysis: state-of-the-art and future challenges. *Nat Neurosci*, 7(5):456–461, May 2004.

A. Diem, G. Gruenert, and P. Dittrich. Evolution and growth of molecular networks for disease classification. In *European Conference on Complex Systems*, September 2012.

A. G. Dimitrov and J. P. Miller. Natural time scales for neural encoding. *Neurocomputing*, 32–33:1027 – 1034, 2000.

P. Dittrich. Chemical computing. In J.-P. Banâtre, P. Fradet, J.-L. Giavitto, and O. Michel, editors, *Unconventional Programming Paradigms*, volume 3566 of *Lecture Notes in Computer Science*, pages 19–32. Springer Berlin Heidelberg, 2005.

G. Escuela, G. Gruenert, and P. Dittrich. Symbol representations and signal dynamics in evolving droplet computers. *Natural Computing*, pages 1–10, 2013.

A. M. Fraser and H. L. Swinney. Independent coordinates for strange attractors from mutual information. *Phys. Rev. A*, 33:1134–1140, Feb 1986.

J. Gorecki, J. Szymanski, and J. N. Gorecka. Realistic parameters for simple models of the belousov–zhabotinsky reaction. *The Journal of Physical Chemistry A*, 115(32): 8855–8859, 2011.

J. Gorecki, J. N. Gorecka, and A. Adamatzky. Information coding with frequency of oscillations in belousov-zhabotinsky encapsulated disks. *Unpublished manuscript*, 2013.

G. Gruenert, J. Szymanski, J. Holley, G. Escuela, A. Diem, B. Ibrahim, A. Adamatzky, J. Gorecki, and P. Dittrich. Multi-scale modelling of computers made from excitable chemical droplets. *International Journal of Unconventional Computing*, 9:237–266, 2013.

J. Holley, A. Adamatzky, L. Bull, B. De Lacy Costello, and I. Jahan. Computational modalities of belousov-zhabotinsky encapsulated vesicles. *Nano Communication Networks*, 2:50–61, 2011a.

J. Holley, I. Jahan, B. Costello, L. Bull, and A. Adamatzky. Logical and arithmetic circuits in belousov zhabotinsky encapsulated discs. *Physical Review E*, 84(5):056110, 2011b.

G. Jetschke. *Mathematik der Selbstorganisation: qualitative Theorie nichtlinearer dynamischer Systeme und gleichgewichtsferner Strukturen in Physik, Chemie und Biologie*. Dt. Verl. d. Wiss., 1989.

S.-H. Jin, P. Lin, and M. Hallett. Linear and nonlinear information flow based on time-delayed mutual information method and its application to corticomuscular interaction. *Clinical Neurophysiology*, 121(3):392 – 401, 2010.

M. Jinguji, M. Ishihara, and T. Nakazawa. Primary process of illumination effect on the tris(bipyridine)ruthenium(2+)-catalyzed belousov-zhabotinskii reaction. *The Journal of Physical Chemistry*, 96(11):4279–4281, 1992.

J. T. Lizier, M. Prokopenko, and A. Y. Zomaya. Local information transfer as a spatiotemporal filter for complex systems. *Phys. Rev. E*, 77:026110, Feb 2008.

W. Maass, T. Natschläger, and H. Markram. Real-time computing without stable states: A new framework for neural computation based on perturbations. *Neural Computation*, 14(11):2531–2560, Nov. 2002.

I. Nemenman, W. Bialek, and R. de Ruyter van Steveninck. Entropy and information in neural spike trains: Progress on the sampling problem. *Phys. Rev. E*, 69:056111, May 2004.

R. Noyes, R. Field, and E. Koros. Oscillations in chemical systems. i. detailed mechanism in a system showing temporal oscillations. *Journal of the American Chemical Society*, 94(4):1394–1395, 1972.

J. Pahle, A. Green, C. J. Dixon, and U. Kummer. Information transfer in signaling pathways: A study using coupled simulated and experimental data. *BMC Bioinformatics*, 9(1):139, 2008.

S. Panzeri and A. Treves. Analytical estimates of limited sampling biases in different information measures. *Network: Computation in Neural Systems*, 7:87–107, 1996.

E. Pereda, R. Q. Quiroga, and J. Bhattacharya. Nonlinear multivariate analysis of neurophysiological signals. *Progress in Neurobiology*, 77(1–2):1 – 37, 2005.

L. Prechelt. Proben1: A set of neural network benchmark problems and benchmarking rules. Technical report, 1994.

R. Q. Quiroga and S. Panzeri. Extracting information from neuronal populations: information theory and decoding approaches. *Nature Reviews Neuroscience*, 10(3):173–185, 2009.

M. S. Roulston. Estimating the errors on measured entropy and mutual information. *Physica D: Nonlinear Phenomena*, 125(3–4):285–294, 1999.

T. Schreiber. Measuring information transfer. *Phys. Rev. Lett.*, 85:461–464, Jul 2000.

C. E. Shannon. A mathematical theory of communication. *Bell System Technical Journal*, 27:379–423 and 623–656, 1948.

R. V. Solé and A. Munteanu. The large-scale organization of chemical reaction networks in astrophysics. *Europhysics Letters*, 68(2):170, 2004.

M. Staniek and K. Lehnertz. Symbolic transfer entropy. *Phys. Rev. Lett.*, 100:158101, Apr 2008.

S. Stepney. Programming unconventional computers: Dynamics, development, self-reference. *Entropy*, 14(10):1939–1952, 2012.

S. P. Strong, R. Koberle, R. R. de Ruyter van Steveninck, and W. Bialek. Entropy and information in neural spike trains. *Phys. Rev. Lett.*, 80:197–200, Jan 1998.

G. Sugihara, R. May, H. Ye, C.-h. Hsieh, E. Deyle, M. Fogarty, and S. Munch. Detecting causality in complex ecosystems. *Science*, 338(6106):496–500, 2012.

J. Szymanski, J. N. Gorecka, Y. Igarashi, K. Gizynski, J. Gorecki, K.-P. Zauner, and M. D. Planque. Droplets with information processing ability. *International Journal of Unconventional Computing*, 7(3):185–200, 2011a.

J. Szymanski, J. N. Gorecka, Y. Igarashi, K. Gizynski, J. Gorecki, K.-P. Zauner, and M. D. Planque. Droplets with information processing ability. *International Journal of Unconventional Computing*, 7(3):185–200, 2011b.

J. Szymanski, J. Gorecki, and M. J. B. Hauser. Chemo-mechanical coupling in reactive droplets. *The Journal of Physical Chemistry C*, 117(25):13080–13086, 2013.

M. Wibral, B. Rahm, M. Rieder, M. Lindner, R. Vicente, and J. Kaiser. Transfer entropy in magnetoencephalographic data: Quantifying information flow in cortical and cerebellar networks. *Progress in Biophysics and Molecular Biology*, 105:80 – 97, 2011.

P. L. Williams and R. D. Beer. Information dynamics of evolved agents. In S. Doncieux, B. Girard, A. Guillot, J. Hallam, J.-A. Meyer, and J.-B. Mouret, editors, *From Animals to Animats 11*, volume 6226 of *Lecture Notes in Computer Science*, pages 38–49. Springer Berlin Heidelberg, 2010a.

P. L. Williams and R. D. Beer. Nonnegative decomposition of multivariate information. *arXiv preprint arXiv:1004.2515*, 2010b.

A. N. Zaikin and A. M. Zhabotinsky. Concentration wave propagation in two-dimensional liquid-phase self-oscillating system. *Nature*, 225(5232):535–537, Feb. 1970.

K. Zauner. Molecular information technology. *Critical Reviews in Solid State and Material Sciences*, 30(1):33–69, 2005.